Vibration and Instability of Third-Order Shear Deformable FGM Sandwich Cylindrical Shells Conveying Fluid

LI Zhihang[1*], *ZHANG Yufei*[2], *WANG Yanqing*[1]

1. Key Laboratory of Structural Dynamics of Liaoning Province, College of Sciences, Northeastern University, Shenyang 110819, P.R. China;

2. School of Aerospace Engineering, Shenyang Aerospace University, Shenyang 110136, P.R. China

(Received 21 December 2021; revised 10 February 2022; accepted 23 February 2022)

Abstract: The vibration and instability of functionally graded material (FGM) sandwich cylindrical shells conveying fluid are investigated. The Navier-Stokes relation is used to describe the fluid pressure acting on the FGM sandwich shells. Based on the third-order shear deformation shell theory, the governing equations of the system are derived by using the Hamilton's principle. To check the validity of the present analysis, the results are compared with those in previous studies for the special cases. Results manifest that the natural frequency of the fluid-conveying FGM sandwich shells increases with the rise of the core-to-thickness ratio and power-law exponent, while decreases with the rise of fluid density, radius-to-thickness ratio and length-to-radius ratio. The fluid-conveying FGM sandwich shells lose stability when the non-dimensional flow velocity falls in 2.1—2.5, which should be avoided in engineering application.

Key words: FGM sandwich shell; fluid; third-order shear deformation shell theory; vibration; stability

CLC number: TB12 **Document code**: A **Article ID**: 1005-1120(2022)01-0047-11

0 Introduction

Pipes conveying fluid are found in numerous industrial applications, in particular in water conservancy project and submarine oil transport[1-2]. For pipes containing fluid, couple vibrations are a major problem due to fluid flow[3-4]. The dynamics of fluid-conveying pipes were extensively reviewed in Refs. [5-7]. One of the earliest studies in the area of dynamics and stability of pipes conveying fluid was proposed by Paidoussis et al.[8]. Zhang et al.[9] investigated the multi-pulse chaotic dynamics of pipes conveying pulsating fluid in parametric resonance. Ding et al.[10] studied the nonlinear vibration isolation of pipes conveying fluid using quasi-zero stiffness characteristics. Tan et al.[11] studied the parametric resonances of pipes conveying pulsating high-speed fluid based on the Timoshenko beam theory. Selmane et al.[12] discussed the effect of flowing fluid on the vibration characteristics of an open, anisotropic cylindrical shell submerged and subjected simultaneously to internal and external flow. Amabili et al.[13] investigated the non-linear dynamics and stability of simply supported, circular cylindrical shells containing inviscid and incompressible fluid flow.

Functionally gradient materials (FGMs) have some prominent advantages such as avoiding crack, avoiding delamination, reducing stress concentration, eliminating residual stress, etc.[14]. Due to these superiorities, vibrations and dynamics stability of structures with FGM properties have attracted much attention[15-21]. Chen et al.[22] studied the free vibration of simply supported, fluid-filled FGM cy-

*Corresponding author, E-mail address: 1800282@mail.neu.edu.cn.

How to cite this article: LI Zhihang, ZHANG Yufei, WANG Yanqing. Vibration and instability of third-order shear deformable FGM sandwich cylindrical shells conveying fluid[J]. Transactions of Nanjing University of Aeronautics and Astronautics, 2022, 39(1): 47-57.

http://dx.doi.org/10.16356/j.1005-1120.2022.01.005

lindrical shells with arbitrary thickness based on the three-dimensional elasticity theory. Sheng et al.[23] studied dynamic characteristics of fluid-conveying FGM cylindrical shells under mechanical and thermal loads. Park et al.[24] presented vibration characteristics of fluid-conveying FGM cylindrical shells resting on Pasternak elastic foundation with an oblique edge.

As one of the most prevalent composite structures applied in aerospace, naval, automotive and nuclear engineering, sandwich structures have attracted tremendous interests from academic and industrial communities[25-33]. Note that the use of FGMs in sandwich shells can mitigate the interfacial shear stress concentration. Thus, dynamics studies of FGM sandwich shells have been carried out by several researchers. Based on the Donnell's shell theory, Dung et al.[34] studied the nonlinear buckling and post-bucking behavior of FGM sandwich circular cylindrical shells. Chen et al.[35] presented the free vibration analysis of FGM sandwich doubly-curved shallow shells under simply supported condition. Fazzolari et al.[36] studied the free vibration of FGM sandwich shells using the Ritz minimum energy method. Tornabene et al.[37] studied the free vibration of rotating FGM sandwich shells with variable thicknesses.

Due to the good thermal insulation of sandwich shells, they can be used as pipelines for transporting petroleum to prevent the paraffin in the crude oil from depositing on the pipe wall after the oil temperature is lowered. The core layer usually uses a material with good heat insulation properties, such as ceramics[38-40]. However, sandwich shells have the interfacial shear stress concentration and are prone to some accidents[41]. Nowadays, FGM sandwich shells can solve this problem and have promising applications in submarine oil transport.

In the present study, we deal with the vibration and instability of FGM sandwich shells conveying fluid. The Navier-Stokes relation is used to describe the fluid pressure acting on the shells. The third-order shear deformation shell theory is used to model the present system. Then, the governing equations and boundary conditions are derived by using the Hamilton's principle. Finally, the frequency and stability results are presented for FGM sandwich shells conveying fluid under various conditions.

1 Theoretical Formulation

1.1 FGM sandwich cylindrical shell

As shown in Fig.1, a fluid-conveying FGM sandwich cylindrical shell made up of three layers, namely, Layer 1, Layer 2 and Layer 3, is considered. The thicknesses of the three layers are h_1, h_2 and h_3, respectively. Layer 2 is the pure ceramic layer, and Layer 1 and Layer 3 are FGM layers. The material properties of Layer 1 and Layer 3 change from pure metal at the outer and inner surfaces to pure ceramic. The dimensions of the shell are denoted by the length L, the middle-surface radius R and the thickness h. A cylindrical coordinate system (x, θ, z) is chosen, where x- and θ-axes define the middle-surface of the shell and z-axis denotes the out-of-surface coordinate.

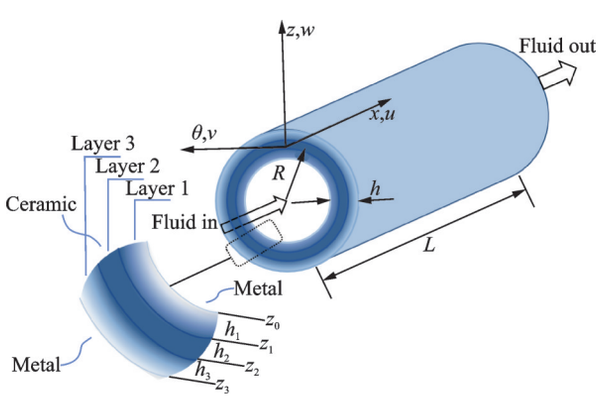

Fig.1 FGM sandwich cylindrical shell conveying fluid

For the FGM sandwich shell, the effective material properties of layer j ($j = 1, 2, 3$) can be expressed as[42]

$$P^{(j)}(z)=(P_c-P_m)V^{(j)}(z)+P_c \tag{1}$$

where P_m and P_c denote the material properties of metal and ceramic, respectively; the volume fraction $V^{(j)}$ ($j = 1, 2, 3$) through the thickness of the sandwich shell follows a power law while it equals unity in the core layer, which reads[43]

$$\begin{cases} V^{(1)}(z)=\left(\dfrac{z-z_0}{z_1-z_0}\right)^k & z\in[z_0, z_1] \\ V^{(2)}(z)=1 & z\in[z_1, z_2] \\ V^{(3)}(z)=\left(\dfrac{z-z_3}{z_2-z_3}\right)^k & z\in[z_2, z_3] \end{cases} \tag{2}$$

where $k\in[0, \infty)$ is the power-law exponent.

Therefore, the Poisson's ratio $\nu^{(j)}(z)$, Young's modulus $E^{(j)}(z)$ and mass density $\rho^{(j)}(z)$ ($j = 1, 2, 3$) of the FGM sandwich shell are expressed as

$$\nu^{(j)}(z)=(\nu_c-\nu_m)V^{(j)}(z)+\nu_m \tag{3}$$

$$E^{(j)}(z)=(E_c-E_m)V^{(j)}(z)+E_m \tag{4}$$

$$\rho^{(j)}(z)=(\rho_c-\rho_m)V^{(j)}(z)+\rho_m \tag{5}$$

where ν_m, ρ_m, E_m are the Poisson ratio, mass density and Young's modulus of metal, respectively; ν_c, ρ_c, E_c the Poisson ratio, mass density and Young's modulus of ceramic, respectively.

1.2 Fluid-shell interaction

The fluid inside the shell is assumed to be incompressible, isentropic and time independent. To simplify the problem, we ignore the influence of the deformation and vibration of the shell on the liquid flow, the shear force transferred from the flow, the flow separation and the Reynold number. The momentum-balance equation for the fluid motion can be described by the well-known Navier-Stokes equation[44]

$$\rho_f\frac{\mathrm{d}\boldsymbol{v}}{\mathrm{d}t}=-\nabla P+\mu\nabla^2\boldsymbol{v}+F_{body} \tag{6}$$

where $\boldsymbol{v}\equiv(v_r, v_\theta, v_x)$ is the flow velocity with components in the r, θ and x directions; P and μ are the pressure and the viscosity of the fluid, respectively; ρ_f is the mass density of the internal fluid; ∇^2 the Laplacian operator and F_{body} the body forces. In this paper, we neglect the action of body forces and consider Newtonian fluid, i.e., the viscosity is time-independent.

At the interface between the fluid and the shell, the velocity of the fluid is equal to the shell in the radial direction. These relationships can be written as[3]

$$v_r=\frac{\mathrm{d}w}{\mathrm{d}t} \tag{7}$$

where r is the distance from the center of the shell to an arbitrary point in the radial direction, and

$$\frac{\mathrm{d}}{\mathrm{d}t}=\frac{\partial}{\partial t}+U\frac{\partial}{\partial x} \tag{8}$$

where U is the mean flow velocity.

Consider the fluid as inviscid. By substituting Eqs.(7, 8) into Eq.(6), the fluid pressure P is obtained as[3]

$$P=\rho_f\left(\frac{\partial^2 w}{\partial t^2}+2U\frac{\partial^2 w}{\partial x\partial t}+U^2\frac{\partial^2 w}{\partial x^2}\right) \tag{9}$$

1.3 Third-order shear deformation theory

According to the third-order shear deformation shell theory, the displacement fields of the fluid-conveying FGM sandwich shell are expressed as[45]

$$\begin{cases} u(x, \theta, z, t)=u_0(x, \theta, t)+ \\ \qquad z\phi_x(x, \theta, t)-c_1z^3\left(\phi_x+\dfrac{\partial w_0}{\partial x}\right) \\ v(x, \theta, z, t)=v_0(x, \theta, t)+ \\ \qquad z\phi_\theta(x, \theta, t)-c_1z^3\left(\phi_\theta+\dfrac{1}{R}\dfrac{\partial w_0}{\partial \theta}\right) \\ w(x, \theta, z, t)=w_0(x, \theta, t) \end{cases} \tag{10}$$

where $c_1=4/3h^2$; u, v and w are the displacements of an arbitrary point of the shell; u_0, v_0 and w_0 the displacements of a generic point of the middle surface; ϕ_x and ϕ_θ the rotations of a normal to the mid-surface about θ and x axes, respectively.

The strain components at a distance z from the mid-plane are[45]

$$\begin{pmatrix}\varepsilon_x\\ \varepsilon_\theta\\ \gamma_{x\theta}\end{pmatrix}=\begin{pmatrix}\varepsilon_x^0\\ \varepsilon_\theta^0\\ \gamma_{x\theta}^0\end{pmatrix}+z\begin{pmatrix}k_x^1\\ k_\theta^1\\ k_{x\theta}^1\end{pmatrix}+z^3\begin{pmatrix}k_x^3\\ k_\theta^3\\ k_{x\theta}^3\end{pmatrix} \tag{11}$$

$$\begin{pmatrix}\gamma_{xz}\\ \gamma_{\theta z}\end{pmatrix}=\begin{pmatrix}\gamma_{xz}^0\\ \gamma_{\theta z}^0\end{pmatrix}+z^2\begin{pmatrix}k_{xz}^2\\ k_{\theta z}^2\end{pmatrix} \tag{12}$$

where

$$\begin{pmatrix}\varepsilon_x^0\\ \varepsilon_\theta^0\\ \gamma_{x\theta}^0\end{pmatrix}=\begin{pmatrix}\dfrac{\partial u_0}{\partial x}\\ \dfrac{1}{R}\dfrac{\partial v_0}{\partial\theta}+\dfrac{w_0}{R}\\ \dfrac{1}{R}\dfrac{\partial u_0}{\partial\theta}+\dfrac{\partial v_0}{\partial x}\end{pmatrix} \tag{13}$$

$$\begin{pmatrix}k_x^1\\ k_\theta^1\\ k_{x\theta}^1\end{pmatrix}=\begin{pmatrix}\dfrac{\partial\phi_x}{\partial x}\\ \dfrac{1}{R}\dfrac{\partial\phi_\theta}{\partial\theta}\\ \dfrac{1}{R}\dfrac{\partial\phi_x}{\partial\theta}+\dfrac{\partial\phi_\theta}{\partial x}\end{pmatrix} \tag{14}$$

$$\begin{pmatrix}k_x^3\\ k_\theta^3\\ k_{x\theta}^3\end{pmatrix}=-c_1\begin{pmatrix}\dfrac{\partial\phi_x}{\partial x}+\dfrac{\partial^2 w_0}{\partial x^2}\\ \dfrac{1}{R}\dfrac{\partial\phi_\theta}{\partial\theta}+\dfrac{1}{R^2}\dfrac{\partial^2 w_0}{\partial\theta^2}\\ \dfrac{1}{R}\dfrac{\partial\phi_x}{\partial\theta}+\dfrac{\partial\phi_\theta}{\partial x}+\dfrac{2}{R}\dfrac{\partial^2 w_0}{\partial x\partial\theta}\end{pmatrix} \tag{15}$$

$$\begin{pmatrix}\gamma_{xz}^0\\ \gamma_{\theta z}^0\end{pmatrix}=\begin{pmatrix}\phi_x+\dfrac{\partial w_0}{\partial x}\\ \phi_\theta+\dfrac{1}{R}\dfrac{\partial w_0}{\partial\theta}\end{pmatrix} \tag{16}$$

$$\begin{pmatrix}k_{xz}^2\\ k_{\theta z}^2\end{pmatrix}=-3c_1\begin{pmatrix}\phi_x+\dfrac{\partial w_0}{\partial x}\\ \phi_\theta+\dfrac{1}{R}\dfrac{\partial w_0}{\partial\theta}\end{pmatrix} \tag{17}$$

where ε_x, ε_θ, $\gamma_{x\theta}$, γ_{xz} and $\gamma_{\theta z}$ are the strains of an arbitrary point; ε_x^0, ε_θ^0, $\gamma_{x\theta}^0$, γ_{xz}^0 and $\gamma_{\theta z}^0$ the strains of a generic point of the middle surface; k_x^1, k_θ^1, $k_{x\theta}^1$, k_x^3, k_θ^3, $k_{x\theta}^3$, k_{xz}^2 and $k_{\theta z}^2$ the curvatures of a generic point of the middle surface.

The relationship between stresses and strains of the fluid-conveying FGM sandwich shell is stated as

$$\begin{Bmatrix}\sigma_x^{(j)}\\ \sigma_\theta^{(j)}\\ \tau_{x\theta}^{(j)}\\ \tau_{xz}^{(j)}\\ \tau_{\theta z}^{(j)}\end{Bmatrix}=\begin{bmatrix}Q_{11}^{(j)} & Q_{12}^{(j)} & 0 & 0 & 0\\ Q_{21}^{(j)} & Q_{22}^{(j)} & 0 & 0 & 0\\ 0 & 0 & Q_{66}^{(j)} & 0 & 0\\ 0 & 0 & 0 & Q_{44}^{(j)} & 0\\ 0 & 0 & 0 & 0 & Q_{55}^{(j)}\end{bmatrix}\begin{Bmatrix}\varepsilon_x\\ \varepsilon_\theta\\ \gamma_{x\theta}\\ \gamma_{xz}\\ \gamma_{\theta z}\end{Bmatrix} \tag{18}$$

where Q_{ij} is given by

$$Q_{11}^{(j)}=\frac{E^{(j)}(z)}{1-v^{(j)}(z)^2},\ Q_{12}^{(j)}=\frac{v^{(j)}(z)E^{(j)}(z)}{1-v^{(j)}(z)^2} \tag{19}$$

$$Q_{21}^{(j)}=\frac{v^{(j)}(z)E^{(j)}(z)}{1-v^{(j)}(z)^2},\ Q_{22}^{(j)}=\frac{E^{(j)}(z)}{1-v^{(j)}(z)^2} \tag{20}$$

$$Q_{44}^{(j)}=Q_{55}^{(j)}=Q_{66}^{(j)}=\frac{E^{(j)}(z)}{2[1+v^{(j)}(z)]} \tag{21}$$

1.4 Governing equations and solution

The strain energy of the FGM sandwich shell can be expressed as

$$\begin{aligned}\Pi_S=&\frac{1}{2}\int_0^{2\pi}\int_0^L\sum_{j=1}^3\int_{z_{j-1}}^{z_j}(\sigma_x^{(j)}\varepsilon_x+\sigma_\theta^{(j)}\varepsilon_\theta+\tau_{x\theta}^{(j)}\gamma_{x\theta}+\tau_{xz}^{(j)}\gamma_{xz}+\tau_{\theta z}^{(j)}\gamma_{\theta z})R\mathrm{d}x\mathrm{d}\theta=\frac{1}{2}\int_0^{2\pi}\int_0^L\Bigg\{\Bigg[\Bigg(N_x\frac{\partial u_0}{\partial x}+\frac{N_{x\theta}}{R}\frac{\partial u_0}{\partial\theta}\Bigg)+\\ &\Bigg(N_{x\theta}\frac{\partial v_0}{\partial x}+\frac{N_\theta}{R}\frac{\partial v_0}{\partial\theta}\Bigg)+\Bigg[Q_{xz}\frac{\partial w_0}{\partial x}+\frac{Q_{\theta z}}{R}\frac{\partial w_0}{\partial\theta}-\frac{N_\theta}{R}w_0-3c_1\Bigg(K_{xz}\frac{\partial w_0}{\partial x}+\frac{K_{\theta z}}{R}\frac{\partial w_0}{\partial\theta}\Bigg)+\\ &c_1\Bigg(P_x^2\frac{\partial^2 w_0}{\partial x^2}+\frac{P_\theta^2}{R^2}\frac{\partial^2 w_0}{\partial\theta^2}+2\frac{P_{x\theta}^2}{R}\frac{\partial^2 w_0}{\partial x\partial\theta}\Bigg)\Bigg]+\Bigg[M_x\frac{\partial\phi_x}{\partial x}+\frac{M_{x\theta}}{R}\frac{\partial\phi_x}{\partial\theta}-Q_{xz}\phi_x+3c_1K_{xz}\phi_x-\\ &c_1\Bigg(P_x\frac{\partial\phi_x}{\partial x}+\frac{P_{x\theta}}{R}\frac{\partial\phi_x}{\partial\theta}\Bigg)\Bigg]+\Bigg[M_{x\theta}\frac{\partial\phi_\theta}{\partial x}+\frac{M_\theta}{R}\frac{\partial\phi_\theta}{\partial\theta}-Q_{\theta z}\phi_\theta+3c_1K_{\theta z}\phi_\theta-c_1\Bigg(P_{x\theta}\frac{\partial\phi_\theta}{\partial x}+\frac{P_\theta}{R}\frac{\partial\phi_\theta}{\partial\theta}\Bigg)\Bigg]\Bigg\}R\mathrm{d}x\mathrm{d}\theta\end{aligned} \tag{22}$$

where the resultant forces N_x, N_θ and $N_{x\theta}$, moments M_x, M_θ and $M_{x\theta}$, shear forces Q_{xz} and $Q_{\theta z}$, and higher-order stress resultants P_x, P_θ, $P_{x\theta}$, K_{xz} and $K_{\theta z}$ are defined by

$$(N_x,\ N_\theta,\ N_{x\theta})=\sum_{j=1}^3\int_{z_{j-1}}^{z_j}(\sigma_x^{(j)},\ \sigma_\theta^{(j)},\ \tau_{x\theta}^{(j)})\mathrm{d}z \tag{23-1}$$

$$(M_x,\ M_\theta,\ M_{x\theta})=\sum_{j=1}^3\int_{z_{j-1}}^{z_j}(\sigma_x^{(j)},\ \sigma_\theta^{(j)},\ \tau_{x\theta}^{(j)})z\mathrm{d}z \tag{23-2}$$

$$(Q_{xz},\ Q_{\theta z})=\sum_{j=1}^3\int_{z_{j-1}}^{z_j}(\tau_{xz}^{(j)},\ \tau_{\theta z}^{(j)})\mathrm{d}z \tag{23-3}$$

$$(P_x,\ P_\theta,\ P_{x\theta})=\sum_{j=1}^3\int_{z_{j-1}}^{z_j}(\sigma_x^{(j)},\ \sigma_\theta^{(j)},\ \tau_{x\theta}^{(j)})z^3\mathrm{d}z \tag{23-4}$$

$$(K_{xz},\ K_{\theta z})=\sum_{j=1}^3\int_{z_{j-1}}^{z_j}(\tau_{xz}^{(j)},\ \tau_{\theta z}^{(j)})z^2\mathrm{d}z \tag{23-5}$$

The kinetic energy of the FGM sandwich shell is written as

$$\begin{aligned}\Pi_T=&\frac{1}{2}\int_V\sum_{j=1}^3\int_{z_{j-1}}^{z_j}\rho(z)\Bigg\{\Bigg[\frac{\partial u_0}{\partial t}+z\frac{\partial\phi_x}{\partial t}-\\ &c_1z^3\Bigg(\frac{\partial\phi_x}{\partial t}+\frac{\partial w_0^2}{\partial x\partial t}\Bigg)\Bigg]^2+\Bigg[\frac{\partial v_0}{\partial t}+z\frac{\partial\phi_\theta}{\partial t}-\\ &c_1z^3\Bigg(\frac{\partial\phi_\theta}{\partial t}+\frac{1}{R}\frac{\partial w_0^2}{\partial\theta\partial t}\Bigg)\Bigg]^2+\Bigg(\frac{\partial w_0}{\partial t}\Bigg)^2\Bigg\}\mathrm{d}V\end{aligned} \tag{24}$$

In addition, the potential energy associated to the fluid pressure is given by[4]

$$\Pi_p = \int_0^{2\pi}\int_0^L P\,R\mathrm{d}x\mathrm{d}\theta \tag{25}$$

By using the Hamilton principle

$$\delta\int_{t_1}^{t_2}\left(\Pi_T-\Pi_S-\Pi_p\right)\mathrm{d}t=0 \tag{26}$$

and then equating the coefficients of δu_0, δv_0, δw_0, $\delta\phi_x$ and $\delta\phi_\theta$ to zero, the motion equations of the fluid-conveying FGM sandwich shell can be obtained as

$$\frac{\partial N_x}{\partial x}+\frac{1}{R}\frac{\partial N_{x\theta}}{\partial\theta}=\bar{I}_1\ddot{u}_0+\bar{I}_2\ddot{\phi}_x-\bar{I}_3\frac{\partial\ddot{w}}{\partial x} \tag{27}$$

$$\frac{\partial N_{x\theta}}{\partial x}+\frac{1}{R}\frac{\partial N_\theta}{\partial\theta}=\tilde{I}_1\ddot{v}_0+\tilde{I}_2\ddot{\phi}_\theta-\tilde{I}_3\frac{1}{R}\frac{\partial\ddot{w}}{\partial\theta} \tag{28}$$

$$\frac{\partial Q_{xz}}{\partial x}+\frac{1}{R}\frac{\partial Q_{\theta z}}{\partial\theta}-\frac{N_\theta}{R}-3c_1\left(\frac{\partial K_{xz}}{\partial x}+\frac{1}{R}\frac{\partial K_{\theta z}}{\partial\theta}\right)+c_1\left(\frac{\partial^2 P_x}{\partial x^2}+\frac{1}{R^2}\frac{\partial^2 P_\theta}{\partial\theta^2}+\frac{2}{R}\frac{\partial^2 P_{x\theta}}{\partial x\partial\theta}\right)=\bar{I}_3\frac{\partial\ddot{u}}{\partial x}+\bar{I}_5\frac{\partial\ddot{\phi}_x}{\partial x}+\tilde{I}_3\frac{1}{R}\frac{\partial\ddot{v}}{\partial\theta}+\tilde{I}_5\frac{1}{R}\frac{\partial\ddot{\phi}_\theta}{\partial\theta}+I_1\ddot{w}-c_1^2I_7\left(\frac{\partial^2\ddot{w}}{\partial x^2}+\frac{1}{R^2}\frac{\partial^2\ddot{w}}{\partial\theta^2}\right)+P \tag{29}$$

$$\frac{\partial M_x}{\partial x}+\frac{1}{R}\frac{\partial M_{x\theta}}{\partial\theta}-Q_{xz}+3c_1K_{xz}-c_1\left(\frac{\partial P_x}{\partial x}+\frac{1}{R}\frac{\partial P_{x\theta}}{\partial\theta}\right)=\bar{I}_2\ddot{u}+\bar{I}_4\ddot{\phi}_x-\bar{I}_5\frac{\partial\ddot{w}}{\partial x} \tag{30}$$

$$\frac{\partial M_{x\theta}}{\partial x}+\frac{1}{R}\frac{\partial M_\theta}{\partial\theta}-Q_{\theta z}+3c_1K_{\theta z}-c_1\left(\frac{\partial P_{x\theta}}{\partial x}+\frac{1}{R}\frac{\partial P_\theta}{\partial\theta}\right)=\tilde{I}_2\ddot{v}+\tilde{I}_4\phi_\theta-\tilde{I}_5\frac{1}{R}\frac{\partial\ddot{w}}{\partial\theta} \tag{31}$$

where the inertias $\bar{I}_i$ and $\tilde{I}_i$ ($i=1,2,3,4,5$) are defined by

$$\bar{I}_1=I_1,\ \tilde{I}_1=I_1+\frac{2}{R}I_2 \tag{32}$$

$$\bar{I}_2=I_2-c_1I_4,\ \tilde{I}_2=I_2+\frac{1}{R}I_3-c_1I_4-\frac{c_1}{R}I_5 \tag{33}$$

$$\bar{I}_3=c_1I_4,\ \tilde{I}_3=c_1I_4+\frac{c_1}{R}I_5 \tag{34}$$

$$\bar{I}_4=I_3-2c_1I_5+c_1^2I_7,\ \tilde{I}_4=I_3-2c_1I_5+c_1^2I_7 \tag{35}$$

$$\bar{I}_5=c_1I_5-c_1^2I_7,\ \tilde{I}_5=c_1I_5-c_1^2I_7 \tag{36}$$

$$(I_1,I_2,I_3,I_4,I_5,I_7)=\sum_{j=1}^{3}\int_{z_{j-1}}^{z_j}\rho^{(j)}(z)(1,z,z^2,z^3,z^4,z^6)\mathrm{d}z \tag{37}$$

By substituting Eq.(23) into Eqs.(27—31), the equations of motion can be rewritten as follows

$$L_1(u_0,v_0,w_0,\phi_x,\phi_\theta)=\bar{I}_1\ddot{u}_0+\bar{I}_2\ddot{\phi}_x-\bar{I}_3\frac{\partial\ddot{w}_0}{\partial x} \tag{38}$$

$$L_2(u_0,v_0,w_0,\phi_x,\phi_\theta)=\tilde{I}_1\ddot{v}_0+\tilde{I}_2\ddot{\phi}_\theta-\tilde{I}_3\frac{1}{R}\frac{\partial\ddot{w}_0}{\partial\theta} \tag{39}$$

$$L_3(u_0,v_0,w_0,\phi_x,\phi_\theta)=\bar{I}_3\frac{\partial\ddot{u}_0}{\partial x}+\bar{I}_5\frac{\partial\ddot{\phi}_x}{\partial x}+\tilde{I}_3\frac{1}{R}\frac{\partial\ddot{v}_0}{\partial\theta}+\tilde{I}_5\frac{1}{R}\frac{\partial\ddot{\phi}_\theta}{\partial\theta}+I_1\ddot{w}_0-c_1^2I_7\left(\frac{\partial^2\ddot{w}_0}{\partial x^2}+\frac{1}{R^2}\frac{\partial^2\ddot{w}_0}{\partial\theta^2}\right)+P \tag{40}$$

$$L_4(u_0,v_0,w_0,\phi_x,\phi_\theta)=\bar{I}_2\ddot{u}_0+\bar{I}_4\ddot{\phi}_x-\bar{I}_5\frac{\partial\ddot{w}_0}{\partial x} \tag{41}$$

$$L_5(u_0,v_0,w_0,\phi_x,\phi_\theta)=\tilde{I}_2\ddot{v}_0+\tilde{I}_4\phi_\theta-\tilde{I}_5\frac{1}{R}\frac{\partial\ddot{w}_0}{\partial\theta} \tag{42}$$

The simply supported boundary condition is considered in this study. It is given by[46]

The solutions to Eqs.(38—42) and Eq.(43) can be separated into a function of time and position as follows[46]

$$\begin{cases}\phi_\theta(0,\theta,t)=\phi_\theta(L,\theta,t)=0\\ N_x(L,\theta,t)=N_x(0,\theta,t)=\\ \qquad M_x(L,\theta,t)=M_x(0,\theta,t)=0\\ v_0(L,\theta,t)=v_0(0,\theta,t)=\\ \qquad w_0(0,\theta,t)=w_0(L,\theta,t)=0\end{cases} \tag{43}$$

$$u_0=\sum_{m=1}^{\infty}\sum_{n=1}^{\infty}u_{mn}(t)\cos(\lambda_m x)\cos(n\theta) \tag{44}$$

$$v_0=\sum_{m=1}^{\infty}\sum_{n=1}^{\infty}v_{mn}(t)\sin(\lambda_m x)\sin(n\theta) \tag{45}$$

$$w_0=\sum_{m=1}^{\infty}\sum_{n=1}^{\infty}w_{mn}(t)\sin(\lambda_m x)\cos(n\theta) \tag{46}$$

$$\phi_x=\sum_{m=1}^{\infty}\sum_{n=1}^{\infty}\phi_{mn}(t)\cos(\lambda_m x)\cos(n\theta) \tag{47}$$

$$\phi_\theta=\sum_{m=1}^{\infty}\sum_{n=1}^{\infty}\bar{\phi}_{mn}(t)\sin(\lambda_m x)\sin(n\theta) \tag{48}$$

where $\lambda_m=m\pi/L$; $u_{mn}(t)$, $v_{mn}(t)$, $w_{mn}(t)$, $\phi_{mn}(t)$ and $\bar{\phi}_{mn}(t)$ represent generalized coordinates.

Substituting Eqs.(44—48) into Eqs.(38—42) yields

$$M_{11}\ddot{u}_{mn}(t)+M_{13}\ddot{w}_{mn}(t)+M_{14}\ddot{\phi}_{mn}(t)+K_{11}u_{mn}(t)+K_{12}v_{mn}(t)+K_{13}w_{mn}(t)+K_{14}\phi_{mn}(t)+K_{15}\bar{\phi}_{mn}(t)=0 \tag{49}$$

$$M_{22}\ddot{v}_{mn}(t)+M_{23}\ddot{w}_{mn}(t)+M_{25}\ddot{\bar{\phi}}_{mn}(t)+K_{21}u_{mn}(t)+K_{22}v_{mn}(t)+K_{23}w_{mn}(t)+K_{24}\phi_{mn}(t)+K_{25}\bar{\phi}_{mn}(t)=0 \tag{50}$$

$$M_{31}\ddot{u}_{mn}(t)+M_{32}\ddot{v}_{mn}(t)+M_{33}\ddot{w}_{mn}(t)+M_{34}\ddot{\phi}_{mn}(t)+M_{35}\ddot{\bar{\phi}}_{mn}(t)+K_{31}u_{mn}(t)+\frac{8\rho_f mU}{L}\sum_{i=1}^{\bar{m}}\frac{i}{m^2-i^2}\dot{w}_{in}(t)+K_{32}v_{mn}(t)+K_{33}w_{mn}(t)+K_{34}\phi_{mn}(t)+K_{35}\bar{\phi}_{mn}(t)=0 \quad (51)$$

$$M_{41}\ddot{u}_{mn}(t)+M_{43}\ddot{w}_{mn}(t)+M_{44}\ddot{\phi}_{mn}(t)+K_{41}u_{mn}(t)+K_{42}v_{mn}(t)+K_{43}w_{mn}(t)+K_{44}\phi_{mn}(t)+K_{45}\bar{\phi}_{mn}(t)=0 \quad (52)$$

$$M_{52}\ddot{v}_{mn}(t)+M_{53}\ddot{w}_{mn}(t)+M_{55}\ddot{\bar{\phi}}_{mn}(t)+K_{51}u_{mn}(t)+K_{52}v_{mn}(t)+K_{53}w_{mn}(t)+K_{54}\phi_{mn}(t)+K_{55}\bar{\phi}_{mn}(t)=0 \quad (53)$$

where $m=1, 2, \cdots, \bar{m}$; $i=1, 2, \cdots, \bar{m}$; $n=1, 2, \cdots, N$; $m \neq i$ and $m \pm i$ are odd numbers. M_{ij} and K_{ij} are integral coefficients.

Eqs. (49—53) can be written in the matrix form as

$$\boldsymbol{M}\ddot{\boldsymbol{X}}+\boldsymbol{C}\dot{\boldsymbol{X}}+\boldsymbol{K}\boldsymbol{X}=\boldsymbol{0} \quad (54)$$

where $\boldsymbol{M}$, $\boldsymbol{C}$, $\boldsymbol{K}$ denote the mass, damping and stiffness matrices, respectively; $\boldsymbol{X}$ is a $5\times\bar{m}\times N$ column vector consisting of $u_{mn}(t)$, $v_{mn}(t)$, $w_{mn}(t)$, $\phi_{mn}(t)$ and $\bar{\phi}_{mn}(t)$.

Eq. (54) is solved in the state space by setting $\boldsymbol{X}=\mathrm{e}^{\Lambda t}\boldsymbol{q}$, which gives the following eigenvalue equation

$$\Lambda\begin{Bmatrix}\boldsymbol{q}\\ \Lambda\boldsymbol{q}\end{Bmatrix}=\begin{bmatrix}\boldsymbol{0} & \boldsymbol{I}\\ -\boldsymbol{M}^{-1}\boldsymbol{K} & -\boldsymbol{M}^{-1}\boldsymbol{C}\end{bmatrix}\begin{Bmatrix}\boldsymbol{q}\\ \Lambda\boldsymbol{q}\end{Bmatrix} \quad (55)$$

where $\{\boldsymbol{q} \quad \Lambda\boldsymbol{q}\}^{\mathrm{T}}$ is the state vector. It should be noted that eigenvalue Λ is a non-zero complex number. The imaginary part of Λ is the frequency and the real part is the damping.

2 Numerical Results and Discussion

The natural frequency is obtained by finding the eigenvalues of the matrix $\begin{bmatrix}\boldsymbol{0} & \boldsymbol{I}\\ -\boldsymbol{M}^{-1}\boldsymbol{K} & -\boldsymbol{M}^{-1}\boldsymbol{C}\end{bmatrix}$. In order to demonstrate the accuracy of the present analysis, a comparison investigation related to a liquid-filled homogenous cylindrical shell is carried out. The used parameters are: $h/R=0.01$, $\rho_f=1\ 000\ \mathrm{kg/m^3}$, iron density $\rho=7\ 850\ \mathrm{kg/m^3}$, $L/R=2$ and $\nu=0.3$. For convenience, the non-dimensional axial flow velocity V is defined as $V=U/\{(\pi/L^2)[D/(\rho h)]^{1/2}\}$ with $D=Eh^3/[12(1-\nu^2)]$; the non-dimensional eigenvalue Ω is introduced as $\Omega=\Lambda/\{(\pi^2/L^2)[D/(\rho h)]^{1/2}\}$. As can be seen from Fig. 2, the result obtained from the current analysis is in good agreement with Amabili et al.[47]. The small difference between them is because the rotational inertia terms $I_2\ddot{\phi}_x$ and $I_2\ddot{\phi}_\theta$ were neglected by Amabili et al.[47]. It is worth mentioning that the real part represents the natural frequency in Ref.[47], which is caused by the use of different solutions.

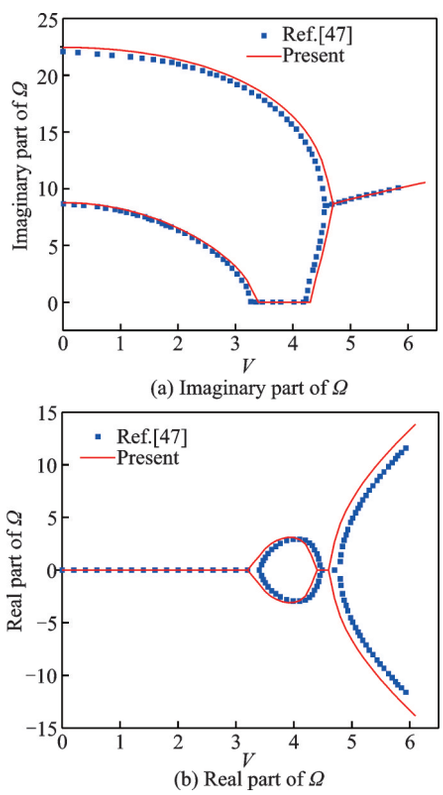

Fig.2 Non-dimensional eigenvalue Ω versus non-dimensional flow velocity V

Next, we investigate the stability and free vibration of FGM sandwich shells conveying fluid. The fluid is considered as crude oil, with a mass density $\rho_f=0.81\ \mathrm{g/cm^3}$[48]. Here, the ceramic and metal forming the FGM sandwich shell shown in Fig.1 are considered as Zirconia and Aluminum, respectively. Their properties are[49]

Aluminum: $E_m=70\ \mathrm{GPa}$, $\nu_m=0.3$, $\rho_m=2\ 707\ \mathrm{kg/m^3}$

Zirconia: $E_c=151\ \mathrm{GPa}$, $\nu_c=0.3$, $\rho_c=$

3 000 kg/m^3

Fig.3 plots the non-dimensional natural frequency versus the circumferential wave number n of FGM sandwich shell conveying fluid. An obvious trend can be found that the frequency first decreases and then increases with the circumferential wave number n. As a result, the fundamental natural frequency of the system happens at mode ($n = 5$, $m = 1$ for $V = 0$). When $V \neq 0$, the modes are coupled for the same circumferential wave number n, and we take $n = 5$ as the representative circumferential wave number for analysis.

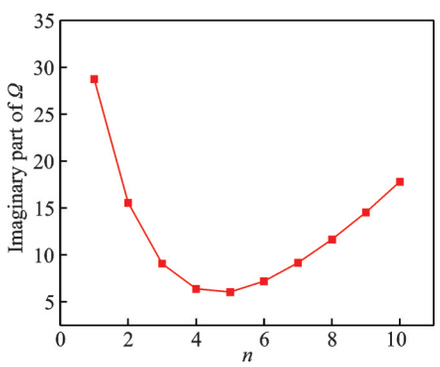

Fig.3 Non-dimensional natural frequency versus circumferential wave number n of FGM sandwich shell conveying fluid (m=1, $L/R = 2.0$, $V = 0$, $k = 1$, $R/h = 80$, $h_2/h = 0.2$)

Fig.4 shows the first two non-dimensional natural frequencies versus the non-dimensional flow velocity of FGM sandwich shell conveying fluid, where $\bar{m} = 2$ is adopted because more axial modes have no effect on the first two natural frequencies. As the flow velocity increases, it is found that both frequencies decrease at first. If the flow velocity reaches certain value, the first frequency vanishes. This velocity is named the critical velocity, at which the system loses its stability due to the divergence via a pitchfork bifurcation. After a small range of instability, the first frequency increases and then coincides with the second frequency, and the system recovers its stability. Moreover, when the flow velocity is between about 2.1—2.5, the fluid-conveying FGM sandwich shell loses stability, which should be avoided in real application.

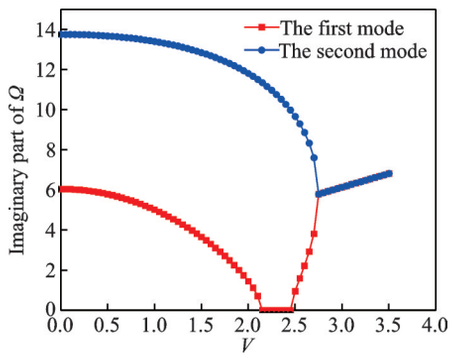

Fig.4 The first two non-dimensional natural frequencies versus non-dimensional flow velocity of FGM sandwich shell conveying fluid ($n = 5$, $L/R = 2.0$, $\bar{m} = 2$, $k = 1$, $R/h = 80$, $h_2/h = 0.2$)

Fig.5 gives the first non-dimensional natural frequency versus the length-to-radius ratio of fluid-conveying FGM sandwich shell with different power-law exponents. It is shown that as the power-law exponent increases, the first non-dimensional natural frequency shows an increasing trend. But the effect of power-law exponent becomes more and more insignificant with increasing length-to-radius ratio. It is also found that as the length-to-radius ratio L/R increases, the first non-dimensional natural frequency decrease. When the length-to-radius ratio is small, the first non-dimensional natural frequency changes obviously. However, when this ratio is large, the first non-dimensional natural frequency is no more sensitive to the length-to-radius ratio.

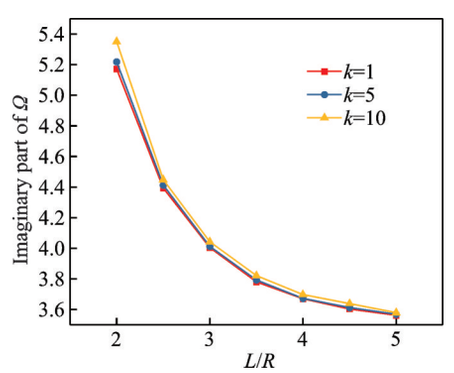

Fig.5 The first non-dimensional natural frequency versus length-to-radius ratio L/R of fluid-conveying FGM sandwich shell with different power-law exponents ($n = 5$, $V = 1$, $\bar{m} = 2$, $R/h = 80$, $h_2/h = 0.2$)

Fig.6 illustrates the first non-dimensional natural frequency versus the radius-to-thickness ratio of fluid-conveying FGM sandwich shell with different power-law exponents. It is shown that as radius-to-thickness ratio R/h increases, the first non-dimensional natural frequency of the fluid-conveying FGM sandwich shell decreases.

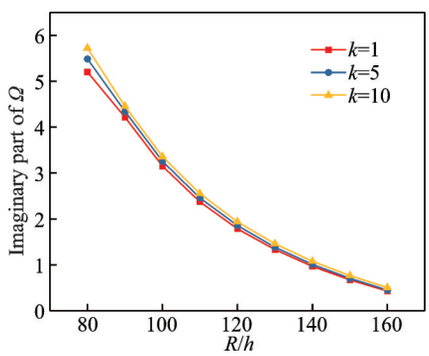

Fig.6 The first non-dimensional natural frequency versus radius-to-thickness ratio R/h of fluid-conveying FGM sandwich shell with different power-law exponents ($n = 5$, $L/R = 2.0$, $\bar{m} = 2$, $V = 1$, $h_2/h = 0.2$)

Fig.7 presents the first non-dimensional natural frequency versus the mass density ρ_f of fluid-conveying FGM sandwich shell with different power-law exponents. The first non-dimensional natural frequency of the fluid-conveying FGM sandwich shell decreases with increasing fluid mass density. This is reasonable because the FGM sandwich shell vibrates as though its mass is increased by the mass of fluid, which is defined as added virtual mass effect.

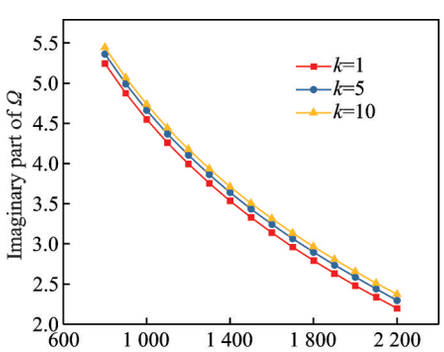

Fig.7 The first non-dimensional natural frequency versus the fluid density ρ_f of fluid-conveying FGM sandwich shell with different power-law exponents ($n = 5$, $L/R = 2.0$, $\bar{m} = 2$, $V = 1$, $h_2/h = 0.2$, $R/h = 80$)

Fig.8 plots the first non-dimensional natural frequency versus the core-to-thickness ratio h_2/h of fluid-conveying FGM sandwich shell with different power-law exponents. It is found that the first non-dimensional natural frequency increases gradually as the core-to-thickness ratio h_2/h increases. This can be understood because the increase of core-to-thickness ratio enhances the stiffness of the structure.

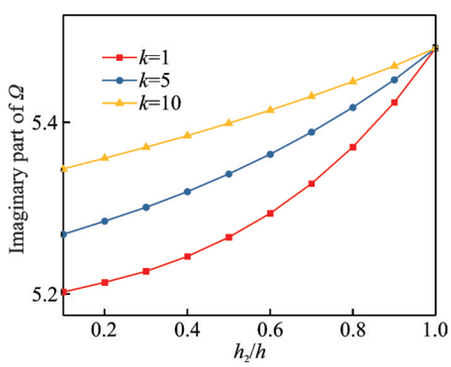

Fig.8 The first non-dimensional natural frequency versus core-to-thickness ratio h_2/h of fluid-conveying FGM sandwich shell with different power-law exponents ($n = 5$, $L/R = 2.0$, $\bar{m} = 2$, $V = 1$, $R/h = 80$)

3 Conclusions

The vibration and instability of FGM sandwich shells conveying fluid are investigated based on the third-order shear deformation shell theory. By using the Hamilton's principle, the governing equations of the present system are derived. Results show that as the flow velocity increases, the natural frequencies of the fluid-conveying FGM sandwich shells decrease at first. When reaching the critical velocity, the first frequency vanishes and the system loses its stability. Moreover, the fluid-conveying FGM sandwich shells lose stability when the non-dimensional flow velocity falls in 2.1—2.5, which should be avoided in submarine oil transport. Besides, the first non-dimensional natural frequency decreases with the rise of fluid density, radius-to-thickness ratio and length-to-radius ratio while increases with the raise of core-to-thickness ratio and power-law exponent. The fluid viscosity has insignificant effect on the first non-dimensional natural frequency of the fluid-conveying FGM sandwich shells.

References

[1] REECE D, BOYLE G J. Insulated pipeline for transporting liquid natural gas: US3547161DA[P]. 1970-12-15.

[2] BERNER D. Hydrates for transport of stranded natural gas[C]//Proceedings of the SPE Annual Technical Conference and Exhibition. USA: Society of Petroleum Engineers, 2003.

[3] WANG L, NI Q. A reappraisal of the computational modelling of carbon nanotubes conveying viscous fluid[J]. Mechanics Research Communications, 2009, 36(7): 833-837.

[4] MOHAMMADI K, BAROUTI M M, SAFARPOUR H, et al. Effect of distributed axial loading on dynamic stability and buckling analysis of a viscoelastic DWCNT conveying viscous fluid flow[J]. Journal of the Brazilian Society of Mechanical Sciences and Engineering, 2019, 41(2): 1-16.

[5] WANG L, DAI H, QIAN Q. Dynamics of simply supported fluid-conveying pipes with geometric imperfections[J]. Journal of Fluids and Structures, 2012, 29: 97-106.

[6] MODARRES-SADEGHI Y, PAïDOUSSIS M. Nonlinear dynamics of extensible fluid-conveying pipes, supported at both ends[J]. Journal of Fluids and Structures, 2009, 25(3): 535-543.

[7] PAÏDOUSSIS M, LI G. Pipes conveying fluid: A model dynamical problem[J]. Journal of Fluids and Structures, 1993, 7(2): 137-204.

[8] PAIDOUSSIS M P, ISSID N. Dynamic stability of pipes conveying fluid[J]. Journal of Sound and Vibration, 1974, 33(3): 267-294.

[9] ZHANG Y, YAO M, ZHANG W, et al. Dynamical modeling and multi-pulse chaotic dynamics of cantilevered pipe conveying pulsating fluid in parametric resonance[J]. Aerospace Science and Technology, 2017, 68: 441-453.

[10] DING H, JI J, CHEN L Q. Nonlinear vibration isolation for fluid-conveying pipes using quasi-zero stiffness characteristics[J]. Mechanical Systems and Signal Processing, 2019, 121: 675-688.

[11] TAN X, DING H. Parametric resonances of Timoshenko pipes conveying pulsating high-speed fluids[J]. Journal of Sound and Vibration, 2020, 485: 115594.

[12] SELMANE A, LAKIS A. Vibration analysis of anisotropic open cylindrical shells subjected to a flowing fluid[J]. Journal of Fluids and Structures, 1997, 11(1): 111-134.

[13] AMABILI M, PELLICANO F, PAÏDOUSSIS M P. Non-linear dynamics and stability of circular cylindrical shells conveying flowing fluid[J]. Computers & Structures, 2002, 80(9/10): 899-906.

[14] JHA D, KANT T, SINGH R. A critical review of recent research on functionally graded plates[J]. Composite Structures, 2013, 96: 833-849.

[15] WANG Y Q, ZU J W. Vibration behaviors of functionally graded rectangular plates with porosities and moving in thermal environment[J]. Aerospace Science and Technology, 2017, 69: 550-562.

[16] WANG Y Q. Electro-mechanical vibration analysis of functionally graded piezoelectric porous plates in the translation state[J]. Acta Astronautica, 2018, 143: 263-271.

[17] CHAI Q, WANG Y Q. Traveling wave vibration of graphene platelet reinforced porous joined conical-cylindrical shells in a spinning motion[J]. Engineering Structures, 2022, 252: 113718.

[18] YE C, WANG Y Q. Nonlinear forced vibration of functionally graded graphene platelet-reinforced metal foam cylindrical shells: Internal resonances[J]. Nonlinear Dynamics, 2021, 104(3): 2051-2069.

[19] WANG Y Q, YE C, ZU J W. Nonlinear vibration of metal foam cylindrical shells reinforced with graphene platelets[J]. Aerospace Science and Technology, 2019, 85: 359-370.

[20] ZHANG W, HAO Y X, GUO X Y, et al. Complicated nonlinear responses of a simply supported FGM rectangular plate under combined parametric and external excitations[J]. Meccanica, 2012, 47(4): 985-1014.

[21] ZHANG W, YANG J, HAO Y. Chaotic vibrations of an orthotropic FGM rectangular plate based on third-order shear deformation theory[J]. Nonlinear Dynamics, 2010, 59(4): 619-660.

[22] CHEN W, BIAN Z, DING H. Three-dimensional vibration analysis of fluid-filled orthotropic FGM cylindrical shells[J]. International Journal of Mechanical Sciences, 2004, 46(1): 159-171.

[23] SHENG G, WANG X. Dynamic characteristics of fluid-conveying functionally graded cylindrical shells under mechanical and thermal loads[J]. Composite

Structures, 2010, 93(1): 162-170.

[24] PARK K J, KIM Y W. Vibration characteristics of fluid-conveying FGM cylindrical shells resting on Pasternak elastic foundation with an oblique edge[J]. Thin-Walled Structures, 2016, 106: 407-419.

[25] SUN C, ZHANG X. Use of thickness-shear mode in adaptive sandwich structures[J]. Smart Materials and Structures, 1995, 4(3): 202.

[26] HAZIZAN M A, CANTWELL W. The low velocity impact response of an aluminium honeycomb sandwich structure[J]. Composites Part B: Engineering, 2003, 34(8): 679-687.

[27] QUEHEILLALT D T, MURTY Y, WADLEY H N. Mechanical properties of an extruded pyramidal lattice truss sandwich structure[J]. Scripta Materialia, 2008, 58(1): 76-79.

[28] FERREIRA A, BARBOSA J, MARQUES A T, et al. Non-linear analysis of sandwich shells: The effect of core plasticity[J]. Computers & Structures, 2000, 76(1/2/3): 337-346.

[29] JING L, WANG Z, ZHAO L. Dynamic response of cylindrical sandwich shells with metallic foam cores under blast loading—Numerical simulations[J]. Composite Structures, 2013, 99: 213-223.

[30] KHARE R K, RODE V, GARG A K, et al. Higher-order closed-form solutions for thick laminated sandwich shells[J]. Journal of Sandwich Structures & Materials, 2005, 7(4): 335-358.

[31] PAIMUSHIN V, BOBROV S. Refined geometric nonlinear theory of sandwich shells with a transversely soft core of medium thickness for investigation of mixed buckling forms[J]. Mechanics of Composite Materials, 2000, 36(1): 59-66.

[32] YANG J S, XIONG J, MA L, et al. Modal response of all-composite corrugated sandwich cylindrical shells[J]. Composites Science and Technology, 2015, 115: 9-20.

[33] VINSON J R. Sandwich structures[J]. Applied Mechanics Reviews, 2001, 54(3): 201-214.

[34] DUNG D V, NGA N T, HOA L K. Nonlinear stability of functionally graded material (FGM) sandwich cylindrical shells reinforced by FGM stiffeners in thermal environment[J]. Applied Mathematics and Mechanics, 2017, 38(5): 647-670.

[35] CHEN H, WANG A, HAO Y, et al. Free vibration of FGM sandwich doubly-curved shallow shell based on a new shear deformation theory with stretching effects[J]. Composite Structures, 2017, 179: 50-60.

[36] FAZZOLARI F A, CARRERA E. Refined hierarchical kinematics quasi-3D Ritz models for free vibration analysis of doubly curved FGM shells and sandwich shells with FGM core[J]. Journal of Sound and Vibration, 2014, 333(5): 1485-1508.

[37] TORNABENE F, FANTUZZI N, BACCIOCCHI M, et al. A numerical investigation on the natural frequencies of FGM sandwich shells with variable thickness by the local generalized differential quadrature method[J]. Applied Sciences, 2017, 7(2): 131.

[38] MOURITZ A P, GELLERT E, BURCHILL P, et al. Review of advanced composite structures for naval ships and submarines[J]. Composite Structures, 2001, 53(1): 21-42.

[39] AN C, DUAN M, ESTEFEN S F. Collapse and buckle propagation of sandwich pipes: A review[C]// Proceedings of the ASME 2013 32nd International Conference on Ocean, Offshore and Arctic Engineering. USA: American Society of Mechanical Engineers Digital Collection, 2013.

[40] FAN J, NJUGUNA J. An introduction to lightweight composite materials and their use in transport structures[M]//Lightweight Composite Structures in Transport. [S.l.]: Elsevier, 2016: 3-34.

[41] LI Q, IU V, KOU K. Three-dimensional vibration analysis of functionally graded material sandwich plates[J]. Journal of Sound and Vibration, 2008, 311(1/2): 498-515.

[42] LANHE W. Thermal buckling of a simply supported moderately thick rectangular FGM plate[J]. Composite Structures, 2004, 64(2): 211-218.

[43] ZENKOUR A. A comprehensive analysis of functionally graded sandwich plates: Part 1—Deflection and stresses[J]. International Journal of Solids and Structures, 2005, 42(18/19): 5224-5242.

[44] WHITE F M, CORFIELD I. Viscous fluid flow[M]. New York: McGraw-Hill, 2006.

[45] REDDY J, LIU C. A higher-order shear deformation theory of laminated elastic shells[J]. International Journal of Engineering Science, 1985, 23(3): 319-330.

[46] CHRISTOFOROU A, SWANSON S. Analysis of simply-supported orthotropic cylindrical shells subject

to lateral impact loads[J]. Journal of Applied Mechanics, 1990, 57(2): 376-382.

[47] AMABILI M, PELLICANO F, PAïDOUSSIS M. Non-linear dynamics and stability of circular cylindrical shells containing flowing fluid. Part I: Stability[J]. Journal of Sound and Vibration, 1999, 225(4): 655-699.

[48] LONGDE S, TONGWEN J, HANLIN X, et al. Unsteady reservoir in Hadson oilfield, Tarim basin[J]. Petroleum Exploration and Development, 2009, 36(1): 62-67.

[49] REDDY J N. Mechanics of laminated composite plates and shells: Theory and analysis[M]. Boca Raton, Florida, USA: CRC Press, 2004.

Acknowledgements This work was supported by the National Natural Science Foundation of China (Nos. 11922205 and 12072201), and the Fundamental Research Fund for the Central Universities (No.N2005019).

Author Mr. **LI Zhihang** received the B.S. degree in solid mechanics from Northeastern University, Shenyang, China, in 2021. He is now pursuing the Ph.D. degree in Wuhan University. His current research interests include vibration and stability of fluid-conveying pipe, and structural health monitoring.

Author contributions Mr. **LI Zhihang** designed the study, complied the models, conducted the analysis, interpreted the results and wrote the manuscript. Prof. **ZHANG Yufei** and Prof. **WANG Yanqing** contributed to the discussion and background of the study. All authors commented on the manuscript draft and approved the submission.

Competing interests The authors declare no competing interests.

(Production Editor: ZHANG Huangqun)

基于三阶剪切变形理论功能梯度夹层输流圆柱壳的振动与稳定性研究

李志航[1], 张宇飞[2], 王延庆[1]

(1.东北大学理学院结构动力学重点实验室,沈阳 110819, 中国; 2.沈阳航空航天大学航天工程学院, 沈阳 110136,中国)

摘要:研究了功能梯度夹层圆柱壳输送流体时的振动与稳定性。使用 Navier-Stokes 方程推导得出作用在功能梯度夹层圆柱壳上的流体动压力。基于三阶剪切变形壳理论,利用哈密顿原理推导得出输流功能梯度夹层圆柱壳的控制方程。本文结果与已有结果的对比研究检验了本文方法的有效性。结果表明:输流功能梯度夹层圆柱壳的固有频率随着芯厚比和幂律指数的增大而增大,随流体密度、径厚比和长径比的增大而减小。当无量纲流速在2.1~2.5时,输流功能梯度夹层圆柱壳将失去稳定,工程应用中应避免这种情况。

关键词:功能梯度夹层圆柱壳;流体;三阶剪切变形壳理论;振动;稳定性